Anion-Responsive Colorimetric and Fluorometric Red-Shift in a Triarylborane Derivative: Dual Role of Phenazaborine as Lewis Acid and Electron Donor

Riku Nakagawa,[a] Leonardo Evaristo de Sousa,[b] Norimitsu Tohnai,[a] Satoshi Minakata,[a] Piotr de Silva,*[b] and Youhei Takeda*[a]

[a] Riku Nakagawa, Prof. Dr. Norimitsu Tohnai, Prof. Dr. Satoshi Minakata, Prof. Dr. Youhei Takeda
Department of Applied Chemistry, Graduate School of Engineering
Osaka University
Yamadaoka 2-1, Suita, Osaka 565-0871, Japan
E-mail: takeda@chem.eng.osaka-u.ac.jp
[b] Dr. Leonardo Evaristo de Sousa, Prof. Dr. Piotr de Silva
Department of Energy Conversion and Storage
Technical University of Denmark
Anker Engelunds Vej 301, 2800 Kongens Lyngby, Denmark
E-mail: pdes@dtu.dk
Supporting information for this article is given via a link at the end of the document.

Abstract

Photophysical modulation of triarylboranes (TABs) through Lewis acid-base interactions is a fundamental approach in sensing anions. Yet, design principles for anion-responsive TABs displaying significant red-shift in absorption and photoluminescence (PL) have remained elusive. Herein, a new strategy for modulating photophysics of TABs in red-shift mode has been presented, endowing a nitrogen-bridged triarylborane (phenazaborine: PAzB) with contradictory dual role as a Lewis acid and an electron donor. Following the strategy, a PAzB derivative connected with an electron-deficient azaaromatic has been developed, and it displays distinct red-shift in absorption and PL in response to an anion. Spectroscopic analyses and quantum chemical calculations have revealed the formation of tetracoordinated borate upon addition of fluoride, narrowing the HOMO-LUMO gap and enhancing charge transfer character in the excited state. This approach has also been demonstrated in solid-state films.

Introduction

Since triorganoboranes (R_3B) possess a vacant $2p_\pi$ orbital on the boron center, they exhibit pronounced Lewis acidity and have thus been widely employed in organic synthesis[1] and catalysis science[2]. Specifically, triarylboranes (TABs), which feature extended π-electron systems as the organic fragment (R = Ar), possess exceptional capability not only for accepting electrons but also for absorbing light in the near-ultraviolet to visible spectrum, owing to their delocalized π-systems spanning the entire molecule. As a result, TABs have been extensively utilized in materials science, finding a variety of applications such as electron transporting materials, nonlinear optical materials, and two-photon-exited fluorescent materials.[3]

In conjunction with intrinsic Lewis acidity and photo-absorbing capability, TABs offer substantial potential for modulating photophysical properties through Lewis acid-base interactions. Complexation of TABs with a Lewis base at the trivalent boron center perturbs its electronic structure, resulting in the breaking of conjugation, structural deformation, and an increase in electron density. By leveraging these phenomena, a wide array of TABs that are capable of sensing Lewis bases have been developed, which are typically classified into three distinct strategies (Figure 1a–c). Of particular importance is the detection of fluoride, as it has significant implications for healthcare and environmental pollution.[4] As a pioneering work in the field of TAB-based colorimetric sensing materials for fluoride, Yamaguchi and Tamao developed tris(9-anthryl)borane.[5] Upon complexation with fluoride, the p_π-π^* conjugation between the anthracene units and the boron center is interrupted, resulting in a change in solution color from orange to colorless. A similar design approach based on the concept of "interrupting conjugation" (Figure 1a) has been applied to π-extended dibenzoboroles, which display a significant blue-shift of fluorescence in the visible light region upon the addition of fluoride and electron-donating solvent such as DMF.[6] Lewis base sensors based on TAB or its polymeric form in a "blue-shift" or "turn-off" mode have been most widely explored.[7–9] The binding event of fluoride to the electrophilic boron center offers an additional avenue for modulating photophysical properties through changing energy transfer (ET) pathway, resulting in a ratiometric change in both absorption and photoluminescence as illustrated in Figure 1b. Takeuchi and Shinkai have developed a conjugate of porphyrin and tris(durene)-cored TAB, with the porphyrin serving as the energy acceptor (EA) and the TAB serving as the energy donor (ED).[10] Inhibiting charge-transfer (CT) from an electron donor (D) to the TAB as an electronic acceptor (A) through complexation with a Lewis base is also commonly utilized

strategy for modulating photophysical properties of TAB compounds, as illustrated in Figure 1c. Conjugated donor-π-acceptor (D–π–A) luminescent compounds, comprising of TAB as the acceptor and triarylamines as the donor, exhibit a blue shift in photoluminescence wavelength upon coordination of fluoride to the boron center.[11,12] This is due to the saturation of the vacant 2p orbital of the boron center upon complexation with fluoride, leading to a "blocking CT" mode and an increase in the intensity of blue-shifted emission from locally excited (LE) state of the donor. For example, Wang et al. reported on a D–π–A TAB compound that has an *N*-(1-naphthyl)phenylamino moiety as the donor and B(mesityl)$_2$ moiety as the acceptor, along with a 1,8-bis(4,4'-biphenyl)naphthalene unit as the π-linker, which exhibited green emission via through-space CT (TSCT) from the donor to the acceptor.[12] The green emission ratiometrically turned to blue with an increase in intensity as a function of the amount of fluoride added, as a result of the inhibition of TSCT (Figure 1c). By incorporating an extended π-system as the linker in the D–π–A system, multiple emission modes can be achieved through Lewis acid-base interactions (Figure 1c).[13] As mentioned above, the majority of known TABs exhibit a "blue-shift" of absorption and PL or "turn-off" of PL upon interaction with a Lewis base, mediated by the disruption of p_π-π* conjugation or the inhibition of CT (Figure 1a–c).[5–14] In sharp contrast, TABs that exhibit a red-shift of absorption and/or PL in response to a Lewis base, such as fluoride and cyanide, have been rarely explored, owing to the lack of rational design principles for such materials.[15] Such anion-responsive TABs would offer new opportunities to detect anions in a complementary manner to hitherto reported materials.

Herein, we disclose the development of TAB compound **1** that displays a distinct red-shift in absorption and PL upon the interaction with a Lewis basic anion, which is enabled by a novel design strategy for narrowing the HOMO-LUMO energy gap and enhancing charge-transfer in the excited state through reversing the intrinsic role of TAB from an electronic acceptor to an electronic donor (as illustrated in Figure 1d).[16] More importantly, the substantial enhancement of CT in the excited states enables the red-shifting of emission even in solid-state host-guest systems, leading to modulation of PL in film state from blue to deep-red and near-infrared (NIR) region.

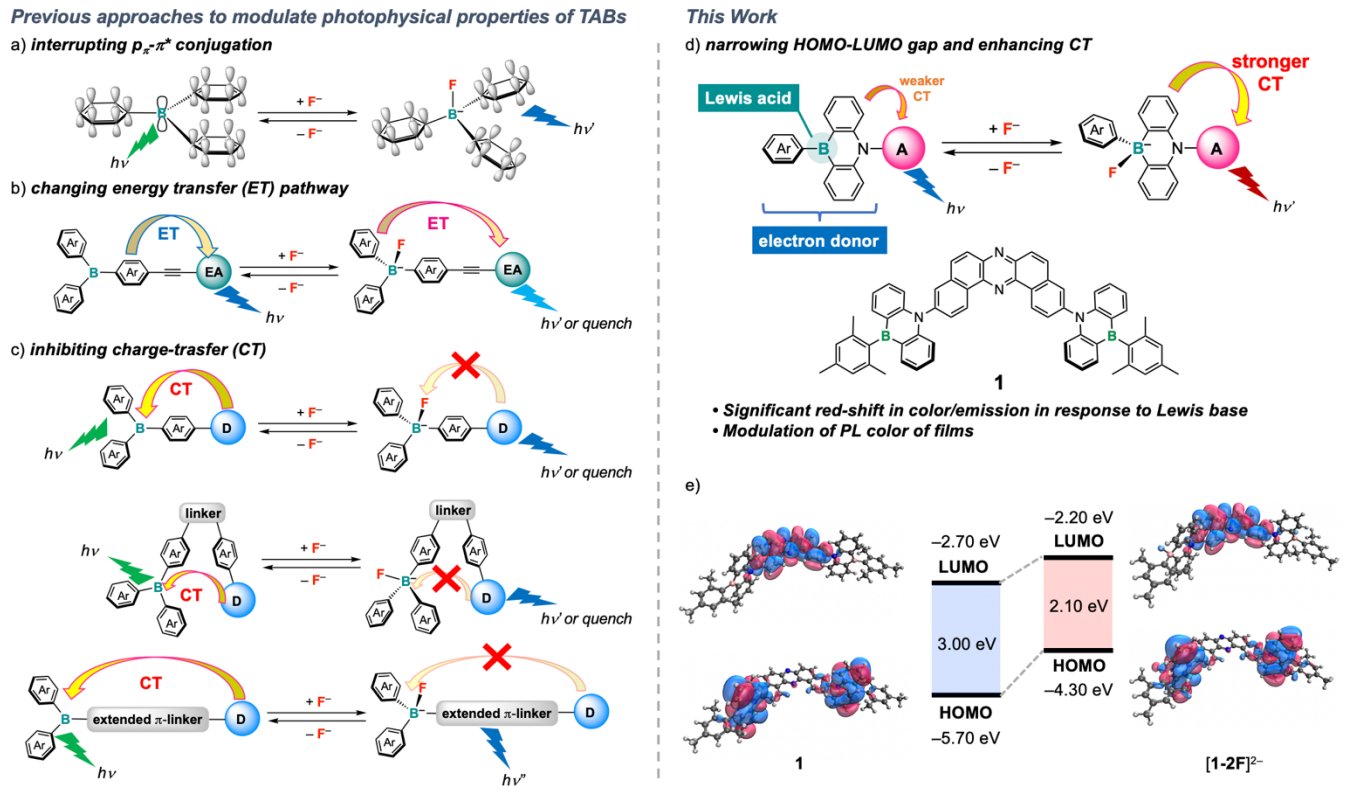

Figure 1. a)–c) Previous and d) our strategies for modulating photophysical properties of TABs with fluoride. e) The HOMO/LUMO energies of **1** and its borate form [**1-2F**]$^{2-}$ estimated by the DFT method calculations.

Results and Discussion

In order to endow a TAB compound with the contradictory dual role as a Lewis acid and an electronic donor, we designed an orthogonally-connected compound comprising of two 1,4-phenazaborines (PAzBs) and dibenzo[*a*,*j*]phenazine (DBPHZ) (**1** in Figure 1d). Given that PAzB possesses a 14π-electron system, it serves as a B,N-analogue of anthracene[17a] and adopts a planar structure.[17b,17i] On one hand, electronic resonance between the nitrogen and boron centers results in ambipolar electronic distribution (–N$^+$=C–C=B$^-$–), thus the PAzB family exhibits distinct physicochemical properties.[17] We envisaged that the structural flatness and ambipolar electronic structure of PAzB would enable its utilization as an electron donor, given that the boron compound is connected with an appropriately

electron-deficient unit. The introduction of a highly electron-deficient functional group, such as ammonium, phosphonium, and diarylboron functionality, on the periphery of PAzB unit drastically enhances K_a values to the order of 10^5 M^{-1}, thereby enabling sufficient capture of fluoride in organic solvents.[18] We focused on DBPHZ as the electron-deficient unit, which exhibits a high electron affinity comparable to that of tris(8-hydroxyquinolinato)aluminium (Alq_3).[19] Additionally, the highly planar structure of DBPHZ and PAzB enables a perpendicular geometry of D and A units in a D–A–D architecture.[20] Thus, we hypothesized that the connection of PAzB and DBPHZ units increases Lewis acidity of the trivalent boron center, due to the disconnection of π conjugation across D and A fragments via orthogonal geometry and a subsequent effective withdrawal of electrons through C–N σ single bond (i.e., inductive effect). The mesityl (Mes) group was selected as an aryl moiety on the boron atom, due to kinetic stabilization of the compound.

The geometry optimization of the designed molecule **1** at the ground state, as determined by quantum chemical calculation based on the density functional theory (DFT) at the LC-ωPBE level with 6-31G(d,p) in THF basis set, revealed that the PAzB adopts a completely planar structure, and the D–A–D molecule adopts a perpendicular geometry as anticipated (Figure 1e; for the detailed description on theoretical calculations, see the SI). It is worth noting that the HOMO and LUMO are localized on the PAzB and DBPHZ unit, respectively (Figure 1e). This suggests that the PAzB serves as the electron donor in this molecular system, as designed. The HOMO-LUMO energy gap for its fluoride adduct $[\mathbf{1\text{-}2F}]^{2-}$ was found to be narrower than that for **1** (Figure 1e), indicating the feasibility of red-shift of absorption spectrum.

The synthesis of D–A–D compound **1** is illustrated in [Eq. (S1–S4)]. The protection of the nitrogen atom of bis(2-bromophenyl)amine (**S1**) with a methoxymethyl (MOM) group was followed by lithium-bromine permutation and trapping the resulting dilithium species with $MesB(OMe)_2$ (**S3**)[21] to afford *N*-MOM phenazaborine (**S4**) [Eq. (S2)]. Deprotection of the N-MOM group furnished donor **S5** in a high yield [Eq. (S3)]. Phenazaborine **S5** was then subjected to a Pd-catalyzed double Buchwald-Hartwig amination with 3,11-dibromo-dibenzo[*a,j*]-phenazine (**S6**),[19] successfully yielding the target D–A–D compound **1** in a high yield (60%) [Eq. (S4)]. The compound **1** was fully characterized by nuclear magnetic resonance (NMR) and infrared (IR) spectroscopy, mass spectrometry (MS), and elemental analysis (EA). Furthermore, all the ^1H and ^{13}C NMR signals were assigned by two-dimensional (2D) NMR spectroscopy (Figure S1–S3).

A single crystal suitable for X-ray crystallographic diffraction analysis was grown from a biphasic solution of *n*-hexane and Et_2O. The unit cell includes two independent molecules (Table S1; one of the molecules are shown in Figure 2). The sum of the C–N–C bond angles [Σ(C–N–C)] and C–B–C bond angles [Σ(C–B–C)] are 360° (Figure 2a), indicating that the PAzB unit is entirely planar. The B–C bond lengths within the 1,4-azaborine ring (1.52–1.53 Å) are also in good agreement with previously reported PAzB compounds.[17] The PAzB and DBPHZ planes are nearly orthogonal to each other (ca. 79° and 89°, Figure 2a), in agreement with theoretical calculation. This would facilitate suppression of electronic conjugation between the donor and acceptor units, thereby increasing the Lewis acidity of the boron center through the C–N connecting bond. With regard to the geometry around the B center, the B-Mes ring is also perpendicular to the PAzB plane (Figure 2a). The U-shaped DBPHZ units are spatially isolated in the packing structure, owing to the perpendicular geometry of the molecule (Figure 2b). In the packing structure, close C•••H and C•••N contacts were found (Figure S4).

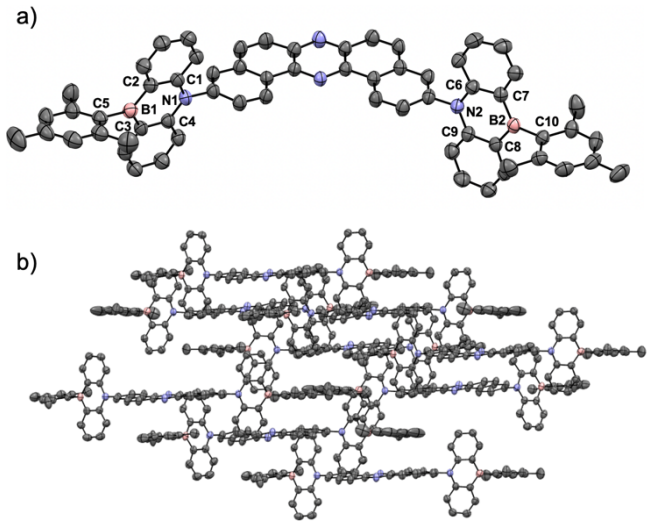

Figure 2. a) Molecular geometry and b) packing structure of **1** in the single crystal. Thermal ellipsoids are set at the 50% probability level. [Σ(C–N1–C)] = 359.9(9)°; [□(C–N2–C)] = 360.0(0)°; [Σ(C–B1–C)] = 359.9(9)°, [Σ(C–B2–C)] = 359.9(1)°; N1–C1 = 1.40(1) Å; C1–C2 = 1.41(0) Å; C2–B1 = 1.53(0) Å; B1–C3 = 1.52(8) A; C3–C4 = 1.40(8) Å; C4–N1 = 1.39(4) Å; N2–C6 = 1.39(1) Å; C6–C7 = 1.41(3) Å; C7–B2 = 1.53(2) Å; B2–C8 = 1.52(9) A; C8–C9 = 1.41(6) Å; C9–N2 = 1.40(6) Å.

To clarify the intrinsic photophysical properties of compound **1** in a diluted solution, UV-Vis absorption and PL spectra were acquired in various solvents (CyH: cyclohexane, Tol: toluene, Diox: 1,4-dioxane, EtOAc: ethyl acetate, THF: tetrahydrofuran, $CHCl_3$: chloroform, Ace: acetone, and DMF: *N,N*-dimethylformamide) (Figure 3 and S5; Table 1 and S2). In all the solvents, compound **1** exhibited a strong, sharp absorption at around λ_{abs} 296 nm, as well as vibronic

structured absorptions between λ_{abs} 350 and 450 nm (Figure 3). Comparison with the absorption spectrum of the individual D and A components and their mixture (D:A = 2:1) in THF (Figure S6 and Table S3) revealed that the longest absorption maximum (λ_{abs} = 419 nm) is attributed to the local excitation of the acceptor (λ_{abs} = 416 nm). A more detailed examination of the absorption spectra revealed the presence of a tail band between 420 to 440 nm, which is not present in the spectrum of an admixture of D and A (D:A = 2:1) (Figure S6). Thus, this observed new band in this regime is ascribed to an intramolecular charge-transfer (ICT) transition from the donor to the acceptor. The simulated absorption spectrum derived from the nuclear ensemble model[22] including 10 excited states displays similar behavior (Figure S10), with a main peak at 366 nm followed by a lower intensity tail at the 430 nm mark. Analysis of the absorption ensemble indicates that the S_0 to S_1 transitions are mainly localized in the acceptor unit, with occasional vibrationally-induced CT states being responsible for the lower energy absorption band (Figure S11).

Although the absorption spectra were not affected by the polarity of the organic solvent, the PL spectrum was drastically red-shifted as a function of solvent polarity, from the blue to the red region (i.e., positive solvatoluminochromism) (Figure 3). The Lippert-Mataga plots clearly show a good linear correlation between the orientation polarizability of the solvent (Δf) and the Stokes shift (the inset graph in Figure 3). The dipole moment in the excited state, estimated from the Lippert-Mataga plot (μ_{ex} = 30.01 Debye), is significantly higher than that in the ground state (μ_g = 2.59 Debye). Furthermore, the emission from **1** is clearly different from the admixture of D and A (D:A = 2:1) (Figure S6), and its spectrum has a Gaussian-type broad shape, suggesting that the D–A–D compound **1** exhibits CT characteristics in the excited state. These results proved that the PAzB serves as donor in the triad system.

Simulations for the emission spectrum of compound **1** proved challenging. Excited state calculations predicted emission from excitations localized in the acceptor unit at around 515 nm. Being a localized excitation, it was insensitive to changes in solvent polarity and thus at odds with experimental results. This indicates that other equilibrium geometry should exist, perhaps due to solvent interactions not captured by standard PCM method. The use of an S_2 optimized geometry to produce a new ensemble revealed, however, the existence of S_1 states with strong CT character. When we consider contributions from these conformations with CT character, we obtain broad Gaussian-like spectra whose peaks move from 429 nm in 1,4-dioxane to 458 nm in THF (Figure S12). This amount of red-shift is smaller than the observed experimentally, which indicates an underestimation of the strength of the CT states of compound **1**. On the other hand, emission rates from simulated spectra are estimated at *ca.* 10^8 s^{-1} ($1.4 \pm 0.5 \times 10^8$ s^{-1} in 1,4-dioxane and 9 $\pm 2 \times 10^7$ s^{-1} in THF), which are consistent with the measured excited state lifetimes (Table S2).

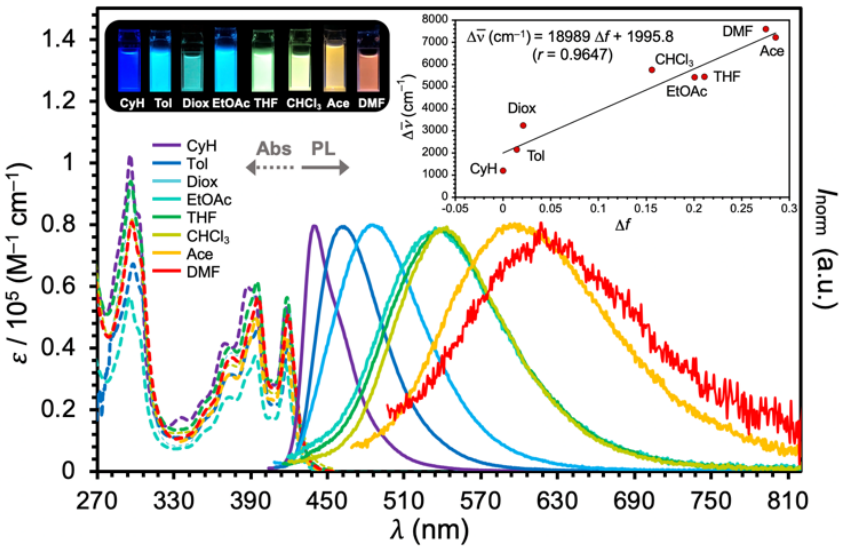

Figure 3. Steady-state UV-Vis and PL spectra of diluted solutions (c = 10^{-5} M) of **1**. The inset photograph and graph show PL of each solution under the irradiation of a UV-lamp (λ_{ex} = 365 nm) and the Lippert-Mataga plot, respectively.

Table 1. Summary of photophysical properties of diluted solution of **1** (c = 10^{-5} M)

solvent	λ_{abs} (nm)	ε ($M^{-1}cm^{-1}$)	λ_{em} (nm)[a]	Φ_{PL}[b]
CyH	388, 418	60000, 53000	440	0.23
Tol	396, 420	46000, 42400	463	0.26
Diox	395, 419	60500, 56500	485	0.23

EtOAc	394, 417	37400, 34300	539	0.11
THF	395, 419	61500, 56300	543	0.14
$CHCl_3$	395, 419	49900, 42700	552	0.13
Ace	394, 417	49500, 44100	597	0.08
DMF	396, 419	51400, 50500	617	0.02

[a] Excited at λ_{exc} = 365 nm. [b] The absolute photoluminescence quantum yield acquired with an integral sphere

Importantly, the addition of a Lewis basic anion (20 equiv) to the THF solution of **1** drastically changed the photophysical properties (Figure 4). To ensure the solubility of anions as a Lewis base in THF, tetrabutylammonium salts (n-$Bu_4N^+A^-$) were employed as the source of Lewis base. When a hard and small or liner-shaped anion such as hydroxide (HO^-), acetate (AcO^-), cyanate (NCO^-), cyanide (CN^-), and fluoride (F^-) was added, the color of the solution containing **1** changed from pale yellow to pink (as seen in the inset photograph in Figure 4a). This colorimetric change is caused by a distinct red-shift of the absorption spectrum as designed (Figure 4a). The absorbance at 252, 395, and 419 nm decreased, while the absorption band between 280 to 360 nm increased. Additionally, a new broadband emerged in the vicinity of 500 nm (Figure 4a), which is ascribed to the difluoride adduct of **1** ($[\mathbf{1}\text{-}\mathbf{2F}]^{2-}[(n\text{-}Bu_4N)_2]^{2+}$). Absorption spectrum simulations of the difluoride adduct $[\mathbf{1}\text{-}\mathbf{2F}]^{2-}$ confirmed the presence of a low intensity band near the 500 nm mark (Figure S13). Further analysis of the ensemble demonstrates that the S_0 to S_1 transition of $[\mathbf{1}\text{-}\mathbf{2F}]^{2-}$ displays strong CT character (Figure S14). The addition of a larger anionic species such as chloride (Cl^-), bromide (Br^-), nitrate (NO_3^-), triflate (TfO^-), and a neutral Lewis base (e.g., Et_3N, pyridine, and DABCO) did not alter the absorption spectrum in any discernible manner (Figure S7a).

In addition to the colorimetric behavior, a significant alteration in PL was observed upon the addition of a Lewis base capable of forming a complex with **1** (Figure 4b) in THF. The green emission of **1** (λ_{em} = 539 nm) turned to orange (λ_{em} = 592 nm) upon the addition of HO^- (Figure 4b). Similar significant red-shift in PL were observed in the cases of addition of AcO^- and NCO^- (Figure 4b). In contrast, fluoride and cyanide resulted in the quenching of emission ("turn-off" of PL) (Figure 4b). Notably, in 1,4-dioxane, a less polar solvent than THF, the PL of **1** displayed a significantly red-shifted emission (peak at 590 nm) upon the addition of TBAF (Figure S8). Fluorescence spectrum simulations (Figure S15) predicted the fluorescence of $[\mathbf{1}\text{-}\mathbf{2F}]^{2-}$ at 625 nm in 1,4-dioxane, in good agreement with experimental results. An estimated emission rate of $6 \pm 1 \times 10^6$ s^{-1} was obtained, a significant reduction when compared with calculated fluorescence rates for compound **1**, which help explain the lower measured quantum yields. Figures 4c and d depict the differences in emission properties and electronic structure of the first excited states of compounds **1** and $[\mathbf{1}\text{-}\mathbf{2F}]^{2-}$ in 1,4-dioxane. For the emission in THF, simulations pointed at a fluorescence peak at 766 nm with a calculated rate of $2.3 \pm 0.2 \times 10^6$ s^{-1} (Figure S15). Emission at such low wavelengths are expected to be strongly quenched by internal conversion, following the energy gap law[23], which could explain why no emission was observed experimentally in this case. Importantly, the addition of BF_3 to the "turn-off" solution recovered the PL in a reversible way ("turn-on") (Figure S9a). The colorimetric change was also reversible upon the same protocol (Figure S9b), indicating the coordination of fluoride to **1** is chemically reversible processes. It is also worth noting that the bases that did not show colorimetric change did not exhibit change in emission either (Figure S7b).

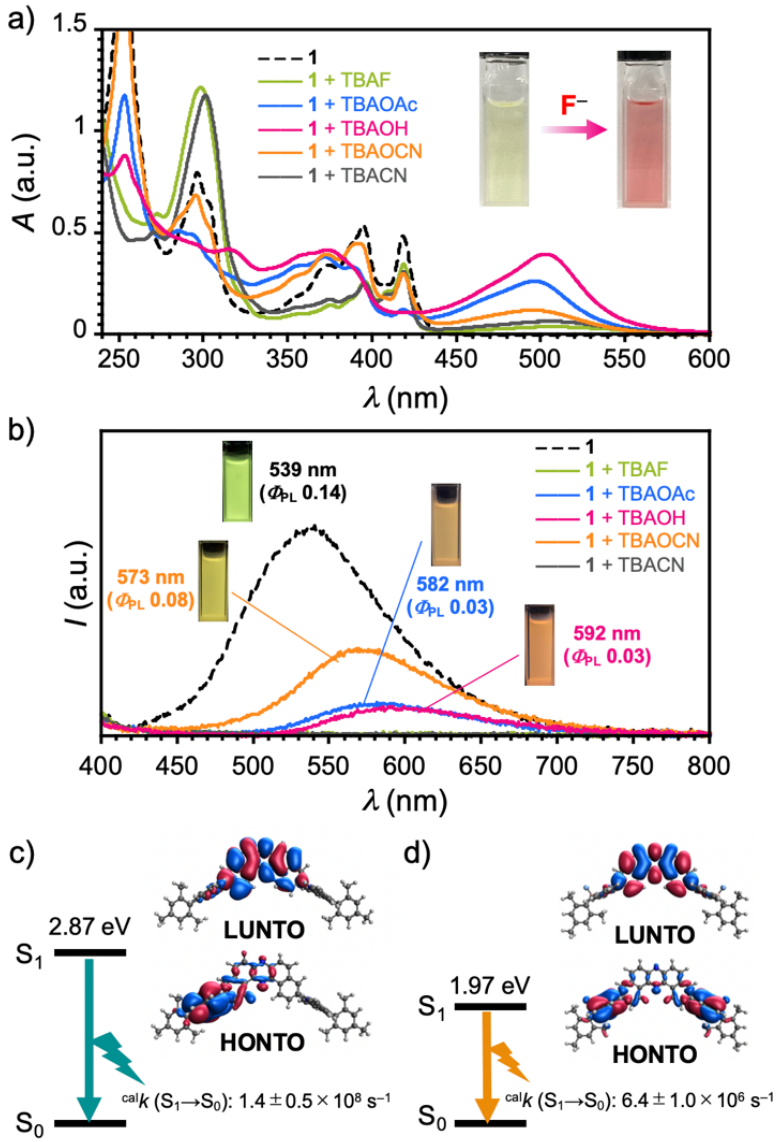

Figure 4. a) UV-vis absorption and b) PL spectra of **1** in the absence and presence of a Lewis base (n-$Bu_4N^+A^-$) in THF. The inset photograph shows the appearance of solutions of **1** (0 eq.) and **1** + TBAF (100 eq.). The HONTO and LUNTO for $S_1 \rightarrow S_0$ transition of c) **1** and d) [**1-2F**]$^{2-}$ in 1,4-dioxane.

The change in chemical species through the addition of a Lewis base was investigated utilizing NMR spectroscopy (Figure 5 and S22–S24). The addition of fluoride (10 equiv of TBAF) as a Lewis base resulted in a significant shift of the aromatic resonances to the higher field region, while preserving the splitting pattern of the signals (Figure 5; the assignment of the ^{1}H and ^{13}C nuclei of [**1-2F**]$^{2-}$[(n-Bu_4N)$_2$]$^{2+}$ was conducted by 2D-NMR spectroscopic analysis. For the details, see the Figure S22–S24 in the SI). It is noteworthy that the magnitude of the signal shift $|\Delta\delta|$ is considerably larger for the ^{1}H nuclei attributed to the donor (**H**^{a}–**H**^{g} 0.21–0.85 ppm) than those for the acceptor (**H**^{h}–**H**^{l} 0.06–0.24 ppm) (for the detailed values, see Table S4). Additionally, it is intriguing to note that only the ^{1}H nuclei of o-CH_3 of the B-Mes group (**H**^{c}) shifted to the lower field, from 2.0 ppm to 2.2 ppm (Figure 5).[24] Given the proximity of the o-CH_3 and boron-coordinated fluoride on the tetra-coordinated boron center (2.40 Å < the sum of Van der Waals radii of H and F: 2.60 Å) in the optimized S_0 geometry, hydrogen bonding H•••F could be operative in the adduct [**1-2F**]$^{2-}$[(n-Bu_4N)$_2$]$^{2+}$ (Figure S16).

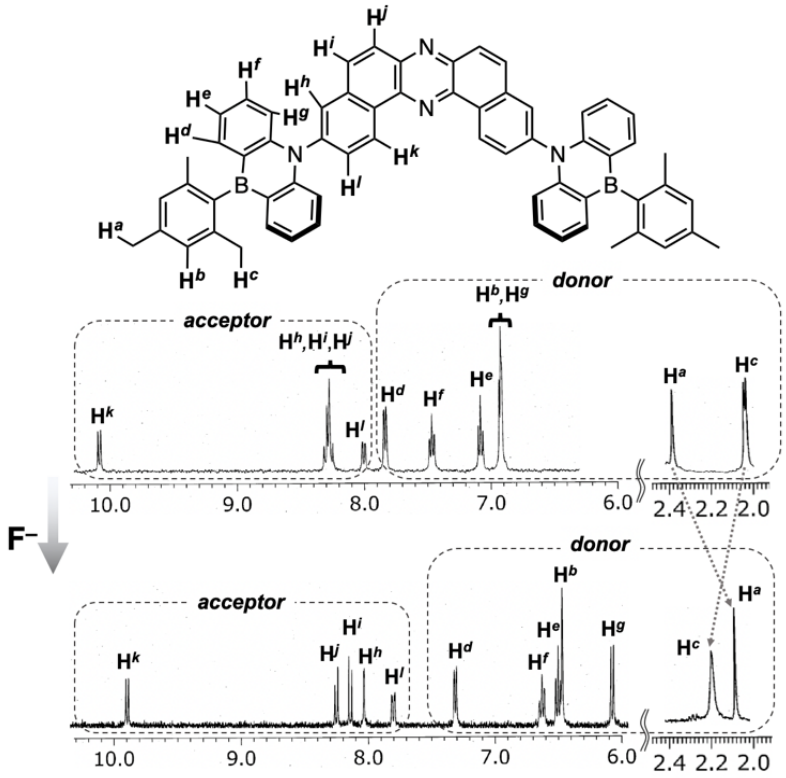

Figure 5. Change in ^{1}H NMR spectrum of **1** upon the addition of fluoride (10 equiv) in THF-d_8.

In order to explore the origin of the substantial upfield-shift of the ^{1}H nuclei in the donor unit, the $NICS_{zz}$ (1) values of the 1,4-azaborine and fused benzene ring in the donor unit were investigated by the DFT method calculations (Figure S17). Whereas the $NICS_{zz}$ (1) value of the 1,4-azaborine ring underwent a marked transformation from –4.26 ppm (aromatic) to +1.00 ppm (non-aromatic) upon coordination with fluoride at the boron center, the $NICS_{zz}$ (1) value of the peripheral benzene ring remained unchanged (–10.63 ppm to –10.16 ppm) (Figure S17). Since the aromaticity of the fused benzene rings did not change upon formation of borate, it can be inferred that the increase in electron density on the donor unit resulting from the action of fluoride led to the significant shift of the donor ^{1}H nuclei to the higher field region. This hypothesis was further supported by the electrostatic potential (ESP) mapping of **1** and $[\mathbf{1}\text{-}\mathbf{2F}]^{2-}[(n\text{-}Bu_4N)_2]^{2+}$ (Figure S18). The presence of a ^{11}B NMR resonance of **1** at +58.5 ppm (Figure S25a) indicated that compound **1** has a planar tricoordinated boron center, which is in consistent with the structure observed by the X-ray crystallographic analysis. Following the addition of fluoride, a new signal appeared at +1.6 ppm, which is indicative of the formation of sp^3-hybridized tetracoordinated borate of phenazaborine $[\mathbf{1}\text{-}\mathbf{2F}]^{2-}[(n\text{-}Bu_4N)_2]^{2+}$ (Figure S25b).[17g]

Cyclic voltammetry enables the assessment of changes in the HOMO/LUMO energy of the D–A–D compound. The cyclic voltammogram of **1** in CH_2Cl_2 revealed a reversible reduction process ($^{red}E_{onset}$ = –1.71 V vs Fc/Fc$^+$) and an irreversible oxidation process ($^{ox}E_{onset}$ = +0.92 V vs Fc/Fc$^+$) (Figure S26a). The HOMO and LUMO, calculated using the redox potential, are –6.02 eV and –3.39 eV, respectively. The LUMO energy is nearly identical to that of DBPHZ (–3.22 eV),[19] supporting the localization of the HOMO and LUMO on the D and A, respectively. The cyclic voltammogram obtained in the presence of fluoride (TBAF) displayed a drastic negative shift in both the reduction potential ($^{red}E_{onset}$ = –2.21 V vs Fc/Fc$^+$) and the oxidation potential ($^{ox}E_{onset}$ = –0.61 V vs Fc/Fc$^+$) when compared with **1** (Figure S26b); the HOMO and LUMO energy of $[\mathbf{1}\text{-}\mathbf{2F}]^{2-}[(n\text{-}Bu_4N)_2]^{2+}$ is estimated to be –4.49 eV and –2.89 eV, respectively. It should be noted that the oxidation potential shifted much more negatively ($\Delta^{ox}E_{onset}$ = –1.53 V) than the reduction potential ($\Delta^{red}E_{onset}$ = –0.50 V). This further supports the coordination of fluoride to the boron center to form borate, which is much more easily oxidized, due to an increase in electron density. The theoretically calculated HOMO/LUMO energy levels of **1** (–5.7 eV/–2.7 eV) and $[\mathbf{1}\text{-}\mathbf{2F}]^{2-}[(n\text{-}Bu_4N)_2]^{2+}$ (–4.3 eV/–2.2 eV) in CH_2Cl_2 (Figure 1d) are qualitatively consistent with the experimental results.

To assess the binding capability of **1** with fluoride, titration experiments were conducted using UV-Vis absorption spectroscopy (Figure 6a). The absorption spectrum undergoes gradual changes as a function of the amount of TBAF added. As the amount of fluoride added increases, the absorbance at 252, 395, and 419 nm decreases (blue arrow in Figure 6a), while the absorbance at 298 nm increases (red arrows in Figure 6a). It is noteworthy that a new absorption band at approximately 500 nm emerged, which should be ascribed to the absorption of $[\mathbf{1}\text{-}\mathbf{2F}]^{2-}[(n\text{-}Bu_4N)_2]^{2+}$– (and/or $[\mathbf{1}\text{-}\mathbf{F}]^-[n\text{-}Bu_4N]^+$). Plotting the difference in absorbance at λ_{abs} 500 nm (ΔA_{500}) against $[F^-]_0/[\mathbf{1}]_0$ yields the titration curve (the inset graph in Figure 6). Although the precise binding constants for fluoride is difficult to determine by the UV-Vis titration, fitting the curve with a non-cooperative 1:2 binding model (Figure S27, $K_1 = 4K_2$)[25,26] estimated K_1 = 3.31 (±0.21) × 10^5 M^{-1} and K_2 = 0.83 (±0.05) × 10^5 M^{-1}. It is noteworthy that these values are comparable to those of bridge-atom-free TABs,[4] demonstrating the well-balanced design for Lewis acidic electron donor. To investigate the

efficacy of the acceptor unit on the nitrogen atom of phenazaborine on the photophysical change in the addition of fluoride, *B*-Mes phenazaborine having an electronically neutral aryl moiety (**N-Ph PAzB**)[27] was titrated with fluoride (Figure 6b, for the synthesis, see [Eq. (S5)]). Upon the addition of fluoride, the vibronic-structured absorptions between 340 and 405 nm ($S_0 \rightarrow S_1$ transition with multi-resonance intramolecular CT character) and a sharp strong absorption at 253 nm ($S_0 \rightarrow S_7$ transition with π–π* character) were decreased, and there was a rise of absorption at 293 nm ($S_0 \rightarrow S_4$ transition of the corresponding fluoroborate with π–π* and CT character) (Figure 6b, Figure S19–S21). As a whole, the absorption spectra were blue-shifted, as commonly observed with TABs.[4] Comparison of the photophysical behavior of **1** and **N-Ph PAzB** clearly showcase that significant red-shift in absorption spectrum upon the addition of fluoride is ascribed to the presence of acceptor unit at the nitrogen atom of phenazaborine structure. The binding constant of **N-Ph PAzB** for fluoride in THF was extracted from the titration curve obtained with the absorbance at $\lambda = 390$ nm (Figure S28) to be $K = 7.03\ (\pm 0.63) \times 10^4\ M^{-1}$, which is one order lower than those of **1**. The drastic increase in binding constants can be attributed to the inductive electron-withdrawing effect of DBPHZ unit as designed. The orthogonal D–A–D geometry further reinforces the inductive effect by shutting off π-conjugation between the D and A, thereby augmenting the Lewis acidity of the PAzB unit and its non-cooperative Lewis acidic characteristics. From these titration experiments, we can deduce that the minimum detection limit of fluoride with **1** is at least 1.52 ppm (5.81 μM) in THF.

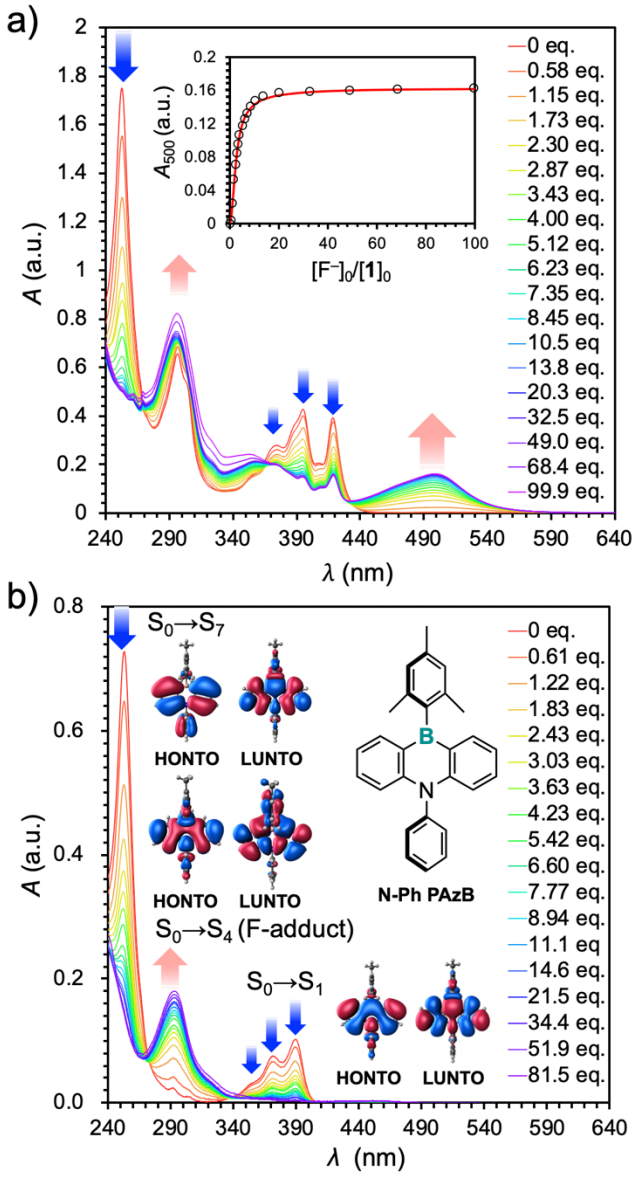

Figure 6. UV-Vis absorption titration of a) **1** (the inset shows titration plots and fitting curve) and b) **N-Ph PAzB** in THF ($c = 10^{-5}$ M) as a function of the amount of TBAF added.

To explore the feasibility of utilizing D–A–D compound **1** for solid-state applications, we examined its solid-state properties. Compound **1** displays green emission ($\lambda_{em} = 511$ nm, Φ_{PL} 0.14) in the solid state (Figure S29). Compared to a dilute solution of **1** in cyclohexane ($\lambda_{em} = 440$ nm, Φ_{PL} 0.23), the emission peak is slightly red-shifted by 3158 cm^{-1} and the photoluminescence quantum yield (PLQY) is lower. This suggests that, despite its orthogonal D–A–D molecular

geometry, some electronic interactions between molecules are operative in the solid state evident by the X-ray crystallographic analysis (Figure S4), leading to slight aggregation-caused quenching (ACQ).

The success in enhancing the CT process of compound **1** in solution through Lewis acid-base interactions prompted us to investigate its solid-state applications. Spin-coating a mixture of **1** (1 wt%) and a polymer matrix in an organic solvent onto a quartz plate, followed by drying under vacuum, resulted in a film (for the detailed procedure, see the SI). The polystyrene (PS) and poly(methyl methacrylate) (PMMA) films containing **1** displayed blue (λ_{em} = 465 nm, Φ_{PL} 0.20) and green (λ_{em} = 535 nm, Φ_{PL} 0.15) emission, respectively (Figure 7a). Similar to solvatochromism in solution, the polar matrix enables emission in the lower energy regime, due to the stabilization of ^{1}CT state in the excited state. Notably, the films fabricated by the mixture of **1**, TBAF, and a matrix displayed a distinct red-shift in PL spectra when compared with polymer films containing only **1** (shift in wavenumber is 5402 cm^{-1} for PS film; 4072 cm^{-1} for PMMA film, Figure 7a), indicating the preservation of fluoroborate [**1**-**2F**]$^{2-}$[(*n*-Bu$_4$N)$_2$]$^{2+}$ even in the matrix. It should be noted that the PL was not quenched in the matrix, probably due to the suppression of molecular vibration in the rigid environment. Additionally, it should be noted that the emission of **1** + TBAF in PMMA film was observed in the deep-red to near-infrared (NIR) region with a sufficient PLQY (Figure 7a). Further modulation of photophysical properties of **1** was implemented by varying the equivalent of TBAF for fabricating films (Figure 7b and Figure S29). The PL spectrum of the film gradually transformed from a single peaked Gaussian-type shape in the blue region to a dual peaked emission as a function of the amount of TBAF added (Figure S30). In the presence of TBAF more than 50 equivalents, the redder emission at around 570 nm red-shifted to 625 nm. The PL intensity ratio of blue to orange emission decreased, and the film containing 500 equivalents of TBAF displayed a single Gaussian-type PL emission at λ_{em} 621 nm (Figure S29). By making use of change in PL spectrum, the emission color of the film is tunable (Figure 7b). Since the emission in the blue region ascribed to D–A–D compound **1** is overlapped with the excitation spectrum of the film fabricated with **1** + TBAF (Figure S31), the Förster resonance energy transfer (FRET) would be operative to lead to significant red-shifted emission from the admixture of **1** and its borates.

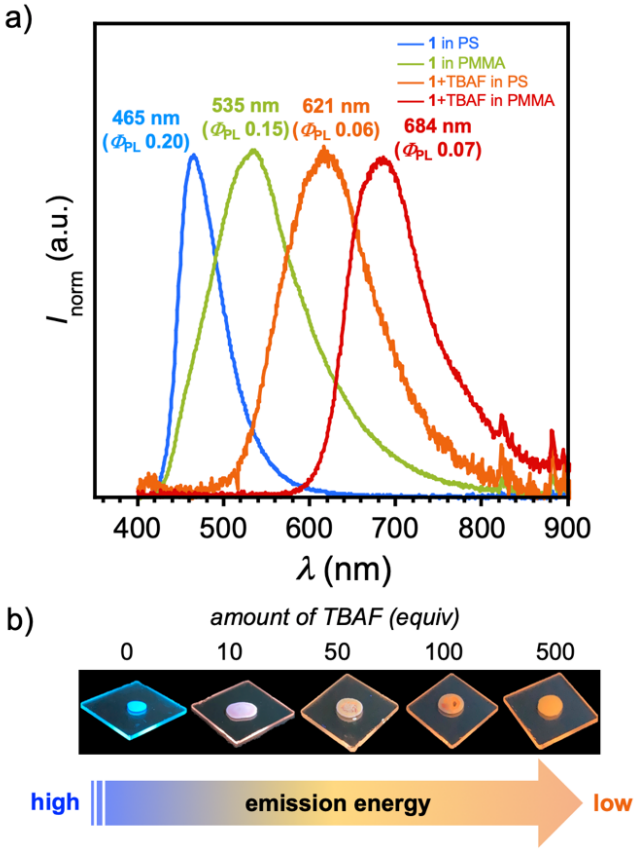

Figure 7. a) PL spectra of **1** (1 wt%) in PS (in sky-blue), **1** in PMMA (in moth green), **1** +TBAF (500 equiv) in PS (in orange), and **1**+TBAF (100 equiv) in PMMA films (λ_{ex} = 365 nm); b) photographs of **1** with varied TBAF content in PS films taken under the irradiation of UV-lamp (λ_{ex} = 365 nm).

Conclusion

In conclusion, a novel triarylborane **1** has been developed that exhibits a red-shift in both its absorption and photoluminescence spectra in response to anionic species. This achievement was accomplished by judiciously reconciling the dualistic properties of phenazaborine as both an electron donor and a Lewis acid. Coordination of anionic

species to the boron center resulted in a marked enhancement of the HOMO energy, which in turn led to a reduction in the HOMO-LUMO gap and the subsequent colorimetric red-shift. Additionally, the strong interaction with fluoride ions facilitates an enhancement in the charge-transfer character of the excited state, leading to a red-shift in photoluminescence in solution and solid state. This novel approach holds promise for modulating the photophysical properties of triarylborane-based organic materials.

Acknowledgements

We acknowledge a Grant-in-Aid for Scientific Research on Innovative Area "Aquatic Functional Materials: Creation of New Materials Science for Environment-Friendly and Active Functions (Area No. 6104)" (JSPS KAKENHI Grant Number JP19H05716 for Y.T.) from the MEXT (Ministry of Education, Culture, Science and Technology, Japan), a Grant-in-Aid for Scientific Research (B) (JSPS KAKENHI Grant Number JP20H02813 for Y.T., 20H02548 for N.T.), a Grant-in-Aid for Challenging Research (Exploratory) (JSPS KAKENHI Grant Number JP21K18960 for Y.T.). P.deS. and L.E.deS. acknowledge a grant no. 2032-00144B from the Independent Research Fund Denmark. Y.T. and S.M. acknowledge NIPPOH CHEMICALS for supplying *N,N*-diiodo-5,5-dimethylhydantoin (DIH).

Keywords: boron • donor-acceptor • charge-transfer • luminescence • sensor

References

[1] A. Suzuki, *Organoboranes in Organic Syntheses*, Hokkaido university Press, Sapporo, **2010**.
[2] J. L. Carden, A. Dasgupta, R. L. Melen, *Chem. Soc. Rev.* **2020**, *49*, 1706–1725.
[3] a) C. D. Entwistle, T. B. Marder, *Angew. Chem. Int. Ed.* **2002**, *41*, 2927–2931; b) C. D. Entwistle, T. B. Marder, *Chem. Mater.* **2004**, *16*, 4574–4585; c) S. Mukherjee, P. Thilagar, *J. Mater. Chem. C* **2016**, *4*, 2647–2662; d) S. M. Berger, T. B. Marder, *Mater. Horiz.* **2022**, *9*, 112–120, and references therein.
[4] a) T. W. Hudnall, C.-W. Chiu, F. P. Gabbaï, *Acc. Chem. Res.* **2009**, *42*, 388–397; b) C. R. Wade, A. E. J. Broomsgrove, S. Aldridge, F. P. Gabbaï, *Chem. Rev.* **2010**, *110*, 3958–3984.
[5] S. Yamaguchi, S. Akiyama, K. Tamao, *J. Am. Chem. Soc.* **2001**, *123*, 11372–11375.
[6] S. Yamaguchi, T. Shirasaka, S. Akiyama, K. Tamao, *J. Am. Chem. Soc.* **2002**, *124*, 8816–8817.
[7] M. Miyata, Y. Chujo, *Polym. J.* **2002**, *34*, 967–969.
[8] A. Sundararaman, M. Victor, R. Varughese, F. Jäkle, *J. Am. Chem. Soc.* **2005**, *127*, 13748–13749.
[9] K. Parab, K. Venkatasubbaiah, F. Jäkle, *J. Am. Chem. Soc.* **2006**, *128*, 12879–12885.
[10] Y. Kubo, M. Yamamoto, M. Ikeda, M. Takeuchi, S. Shinkai, S. Yamaguchi, K. Tamao, *Angew. Chem. Int. Ed.* **2003**, *42*, 2036–2040; *Angew. Chem.* **2003**, *115*, 2082–2086.
[11] a) Z.-Q. Liu, M. Shi, F.-Y. Li, Q. Fang, Z.-H. Chen, T. Yi, C.-H. Huang, *Org. Lett.* **2005**, *7*, 5481–5484; b) M.-S. Yuan, Z.-Q. Liu, Q. Fang, *J. Org. Chem.* **2007**, *72*, 7915–7922.
[12] a) X. Y. Liu, D. R. Bai, S. Wang, *Angew. Chem. Int. Ed.* **2006**, *45*, 5475–5478; *Angew. Chem.* **2006**, *118*, 5601–5604; b) D.-R. Bai, X.-Y. Liu, S. Wang, *Chem. Eur. J.* **2007**, *13*, 5713–5723.
[13] G. Zhou, M. Baumgarten, K. Müllen, *J. Am. Chem. Soc.* **2008**, *130*, 12477–12484.
[14] a) S. Solé, F. P. Gabbaï, *Chem. Commun.* **2004**, *4*, 1284–1285; b) M. Melaimi, F. P. Gabbaï, *J. Am. Chem. Soc.* **2005**, *127*, 9680–9681; c) A. Sundararaman, K. Venkatasubbaiah, M. Victor, L. N. Zakharov, A. L. Rheingold, F. Jäkle, *J. Am. Chem. Soc.* **2006**, *128*, 16554–16565; d) T. W. Hudnall, M. Melaïmi, F. P. Gabbaï, *Org. Lett.* **2006**, *8*, 2747–2749; e) S.-B. Zhao, T. McCormick, S. Wang, *Inorg. Chem.* **2007**, *46*, 10965–10967; f) Y. Sun, N. Ross, S.-B. Zhao, K. Huszarik, W.-L. Jia, R.-Y. Wang, D. Macartney, S. Wang, *J. Am. Chem. Soc.* **2007**, *129*, 7510–7511; g) T. W. Hudnall, F. P. Gabbaï, *J. Am. Chem. Soc.* **2007**, *129*, 11978–11986; h) C.-W. Chiu, Y. Kim, F. P. Gabbaï, *J. Am. Chem. Soc.* **2009**, *131*, 60–61; i) Y. Kim, F. P. Gabbaï, *J. Am. Chem. Soc.* **2009**, *131*, 3363–3369; j) T. Matsumoto, C. R. Wade, F. P. Gabbaï, *Organometallics* **2010**, *29*, 5490–5495; k) H. Zhao, F. P. Gabbaï, *Organometallics* **2012**, *31*, 2327–2335; l) K. C. Song, K. M. Lee, N. Van Nghia, W. Y. Sung, Y. Do, M. H. Lee, *Organometallics* **2013**, *32*, 817–823; m) D.-M. Chen, S. Wang, H.-X. Li, X.-Z. Zhu, C.-H. Zhao, *Inorg. Chem.* **2014**, *53*, 12532–12539; n) A. L. Brazeau, K. Yuan, S.-B. Ko, I. Wyman, S. Wang, *ACS Omega* **2017**, *2*, 8625–8632; o) P. Li, D. Shimoyama, N. Zhang, Y. Jia, G. Hu, C. Li, X. Yin, N. Wang, F. Jäkle, P. Chen, *Angew. Chem. Int. Ed.* **2022**, *61*, e202200612; *Angew. Chem.* **2022**, *134*, e202200612.
[15] a) T. Neumann, Y. Dienes, T. Baumgartner, *Org. Lett.* **2006**, *8*, 495–497; b) C. R. Wade, F. P. Gabbaï, *Dalton Trans.* **2009**, 9169–9175; c) H. Li, F. Jäkle, *Angew. Chem. Int. Ed.* **2009**, *48*, 2313–2316; *Angew. Chem.* **2009**, *121*, 2349–2352; d) C. A. Swamy P, R. N. Priyanka, S. Mukherjee, P. Thilagar, *Eur. J. Inorg. Chem.* **2015**, *2015*, 2338–2344; e) G. R. Kumar, S. K. Sarkar, P. Thilagar, *Chem. Eur. J.* **2016**, *22*, 17215–17225; f) R. E. Messersmith, S. Yadav, M. A. Siegler, H. Ottosson, J. D. Tovar, *J. Org. Chem.* **2017**, *82*, 13440–13448; g) G. Turkoglu, M. E. Cinar, T. Ozturk, *Eur. J. Org. Chem.* **2017**, *2017*, 4552–4561.
[16] In the same timeline with our work, Danos and Zysman-Colman et al. independently reported that phenazaborine serves as a weak electron donor in a donor–acceptor conjugated emitter: S. Pagidi, S. Kuila, K. Stavrou, A. Danos, A. Slawin, A. Monkman, E. Zysman-Colman, *ChemRxiv preprint* **2022**, DOI: 10.26434/chemrxiv-2022-jb4v0.
[17] a) P. M. Maitlis, *J. Chem. Soc.* **1961**, 425–429; b) M. Kranz, F. Hampel, T. Clark, *J. Chem. Soc. Chem. Commun.* **1992**, 1247–1248; c) T. Agou, J. Kobayashi, T. Kawashima, *Org. Lett.* **2006**, *8*, 2241–2244; d) T. Agou, J. Kobayashi, T. Kawashima, *Chem. Commun.* **2007**, 3204–3206; e) T. Agou, T. Kojima, J. Kobayashi, T. Kawashima, *Org. Lett.* **2009**, *11*, 3534–3537; f) T. Agou, M. Sekine, J. Kobayashi, T. Kawashima, *Chem. Eur. J.* **2009**, *15*, 5056–5062; g) T. Agou, M. Sekine, J. Kobayashi, T. Kawashima, *Chem. Commun.* **2009**, 1894–1896; h) T. Agou, H. Arai, T. Kawashima, *Chem. Lett.* **2010**, *39*, 612–613; i) Y. Ishikawa, K. Suzuki, K. Hayashi, S.-Y. Nema, M. Yamashita, *Org. Lett.* **2019**, *21*, 1722–1725.
[18] T. Agou, J. Kobayashi, T. Kawashima, *Inorg. Chem.* **2006**, *45*, 9137–9144.
[19] Y. Takeda, M. Okazaki, S. Minakata, *Chem. Commun.* **2014**, *50*, 10291–10294.
[20] a) P. Data, P. Pander, M. Okazaki, Y. Takeda, S. Minakata, A. P. Monkman, *Angew. Chem. Int. Ed.* **2016**, *55*, 5739–5744; *Angew. Chem.* **2016**, *128*, 5833–5838; b) H. F. Higginbotham, M. Okazaki, P. de Silva, S. Minakata, Y. Takeda, P. Data, *ACS Appl. Mater. Interfaces* **2021**, *13*, 2899–2907.

[21] J. A. Knöller, G. Meng, X. Wang, D. Hall, A. Pershin, D. Beljonne, Y. Olivier, S. Laschat, E. Zysman-Colman, S. Wang, *Angew. Chem. Int. Ed.* **2020**, *59*, 3156–3160; *Angew. Chem.* **2020**, *132*, 3181–3185.
[22] L. E. de Sousa, P. de Silva, *J. Chem. Theory Comput.* **2021**, *17*, 5816–5824.
[23] K. F. Freed, *Acc. Chem. Res.* **1978**, *11*, 74–80.
[24] T. Agou, J. Kobayashi, Y. Kim, F. P. Gabbaï, T. Kawashima, *Chem. Lett.* **2007**, *36*, 976–977.
[25] P. Thordarson, *Chem. Soc. Rev.* **2011**, *40*, 1305–1323.
[26] http://app.supramolecular.org/bindfit/
[27] M. Ando, M. Sakai, N. Ando, M. Hirai, S. Yamaguchi, *Org. Biomol. Chem.* **2019**, *17*, 5500–5504.

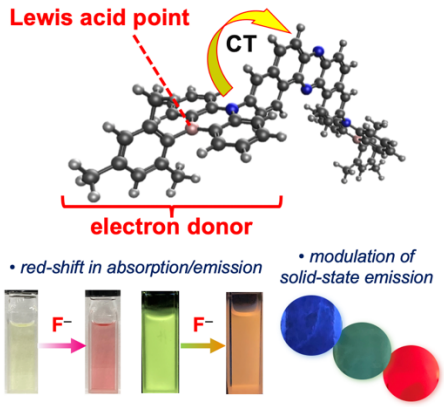

Based on a novel strategy for modulating photophysical properties by balancing contradictory role of phenazaborine as a Lewis acid and an electron donor, an anion-responsive triarylborane compound has been developed. The developed compound displayed significant red-shift in absorption and photoluminescence in solution. This approach has also been successfully applied to modulation of emission color in polymer films.